Experimental Campaign for Dynamic Characterization of a Laboratory-Scale Structure

Matteo Brambilla[1], Vasilis Dertimanis[2], Eleni Chatzi[2], Paolo Chiariotti[1], and Alfredo Cigada[1]

[1]Department of Mechanical Engineering, Politecnico di Milano, Milan, Italy
[2]Institute of Structural Engineering, ETH Zürich, Zürich, Switzerland

1 Introduction

This document presents the dataset obtained from a dynamic testing campaign on a laboratory-scale model of a four-story building. The experiments were conducted at the Institute of Structural Engineering (IBK) at ETH Zürich, as part of a joint collaboration between the Structural Mechanics and Monitoring Group at ETH Zürich and the Measurements and Experimental Techniques Group at Politecnico di Milano.
The structure has an overall height of approximately 1.2 meters, with each floor featuring a square cross-section measuring 0.52 meters. Its geometry is described in detail in [1] and [2]. The model is mounted on a six-degree-of-freedom hydraulic shaking table (hereafter referred to as the *hexapod*) to simulate earthquake-induced vibrations. Due to its shear-dominant behavior, the structure is highly sensitive to lateral (x, y) excitations while remaining stiff in the vertical (z) direction. As a result, the dataset primarily captures x-y directional vibrations, with vertical movements being negligible within the frequency range of up to 20 Hz.
The test campaign considers two structural states:

- **Baseline (b)**: the structure is tested in an undamaged (healthy) condition.
- **Damaged (d)**: a structural modification is introduced with the purpose of reflecting damage, as explained in Section 4.

The experimental campaign consists of two main phases:

1. **Impact testing:** during these tests, the hexapod remained idle. The objective was to characterize the structure using Experimental Modal

Analysis (EMA). Input forces were applied with a modal impact hammer (equipped with a super-soft rubber head), while output accelerations were recorded using six piezoelectric accelerometers (Table 1). A roving accelerometer configuration was employed for the measurements (Table 4). Further details on this testing phase, which was conducted exclusively in the b-state, are provided in Section 3.

2. **Dynamic tests under random excitation:** the hexapod was driven within a specified frequency range using a random excitation profile applied at three distinct root mean square (RMS) levels: *low*, *medium*, and *high*. Each RMS level was combined with a principal excitation direction—either along the x-axis, the y-axis, or simultaneously along both x and y axes—resulting in a total of 17 tests, as summarized in Table 6. This phase, aimed at simulating operational conditions, comprised the following two steps:

   i) Application of random excitations at varying amplitude levels and directions to evaluate the structure's linearity, conducted in the baseline (b) state.

   ii) Application of random excitations at a fixed amplitude and direction, with repeated measurements at different sensor locations. This step was performed first in the baseline (b) state and subsequently in the damaged (d) state.

This document presents the essential information required for effective use of the collected dataset, including details on the test procedures, sensor specifications, setup configurations, and dataset organization.
An unscaled schematic representation of the structure is shown in Figure 1, together with the selected reference coordinate system. The 32 numerical labels in Figure 1a correspond to the cubic joints connecting the columns and floors, which serve as nodal target positions for sensor placement. In the front view of the structure (Figure 1b), the cubic joints are depicted at an enlarged scale for clarity.

2 Measurement Setup

Throughout the test campaign, an eight-channel high-speed digital acquisition (DAQ) system was used in conjunction with various piezoelectric sensors. These sensors recorded the output acceleration response and, during the EMA phase, further captured the input excitation force. The DAQ configurations for the two testing phases are summarized in Table 1 and Table 2, respectively.

1. **Impact testing for EMA.** The digital acquisition system was configured as detailed in Table 1 to record both the input excitation force and the corresponding output acceleration response. The roving accelerometer test sequence is summarized in Table 4 and further described in Section 3.

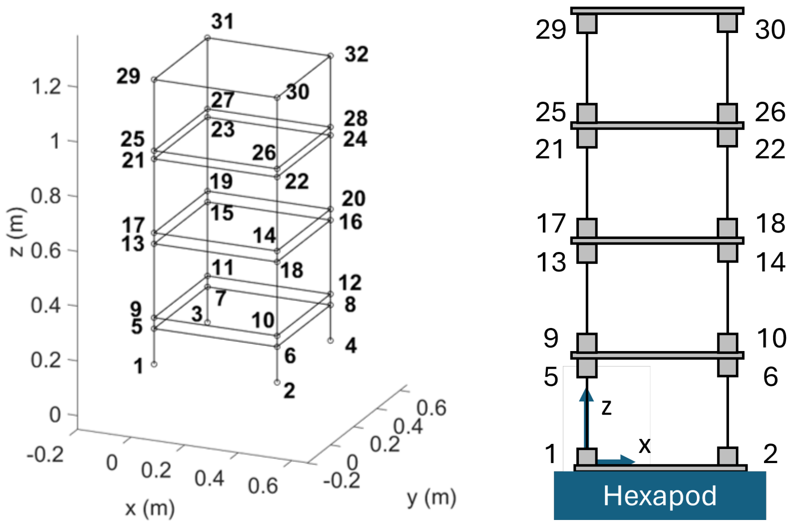

(a) (b)

Figure 1: Schematic representation of the four-story structure under investigation. (a) A three-dimensional view highlighting the 32 nodal positions for sensor placement relative to the reference coordinate system. (b) Front view, with cubic joints exaggerated in scale for clarity.

2. **Random excitation tests.** In addition to the accelerometer setup detailed in Table 2, the cubic joints shown in Figure 1b served as reference points for displacement measurements. These measurements were performed simultaneously with the acceleration recordings using a dynamic measurement machine (DMM), specifically the Optotrack Certus HD model by NDI. The DMM tracked displacements along the three principal directions x, y, z for 16 selected cubic joints visible in the front view of Figure 1b, namely nodes 1, 2, 5, 6, 9, 10, 13, 14, 17, 18, 21, 22, 25, 26, 29, 30.

   It should be noted that, during each test, data acquisition from the piezoelectric accelerometers and the DMM was conducted independently; the two systems did not share a common trigger signal or master sampling frequency. Further details are provided in Section 4.

3 Phase 1 of 2: Impact Testing

The sensor configuration for impact testing is detailed in Table 1. Each accelerometer pair recorded acceleration responses along the x- and y-directions at a single cubic nodal point, as illustrated in Figure 1. The input excitation was applied at nodal point 29, designated as the driving point (DP). As the tests

Table 1: Channel configuration for dynamic tests with impulse excitation. The first column lists the *channel* (Ch.) numbers, while the second column provides the *labels* assigned to each channel in the dataset. The third and fourth columns specify the *sensor model* and its *serial number* (SN), respectively. The fifth column reports the nominal *sensitivity* of each sensor. The sixth column, *Role*, indicates the sensor's position, either as a fixed driving point (DP) or a roving node (N1, N2). The hammer force is recorded in channel 8, labeled as Input. The hammer is equipped with a soft, rubber-made (red) head, model PCB-084C11. For completeness, the role of each sensor is also detailed in Table 4.

Ch.	Label	Sensor model	SN	Sensitivity	Role
1	A	PCB-352C33	LW184506	10.2 $mV/m/s^2$	DP (x)
2	B	PCB-352C33	LW184373	10.2 $mV/m/s^2$	DP (y)
3	C	PCB-333B40	55350	51 $mV/m/s^2$	N1 (x)
4	D	PCB-333B40	55354	51 $mV/m/s^2$	N1 (y)
5	E	PCB-333B40	55353	51 $mV/m/s^2$	N2 (x)
6	F	PCB-333B40	55351	51 $mV/m/s^2$	N2 (y)
7	-	-	-	-	-
8	HAMMER	PCB-086C03	LW41330	2.25 mV/N	Input

Table 2: Channel configuration for acceleration measurements under random excitation. The first column lists the *channel* numbers, while the second column provides the *labels* assigned to each channel as reported in the dataset. The third and fourth columns specify the *sensor model* and its *serial number* (SN), respectively. The fifth column reports the nominal *sensitivity* of each sensor. Sensor placements for different configurations are detailed in Table 5 and illustrated in Figure 2. A triaxial accelerometer, G, is consistently positioned on the ground, measuring hexapod acceleration, with its x- and y-direction components recorded as Gx and Gy, respectively.

Channel	Label	Sensor model	SN	Sensitivity
1	A	PCB-352C33	LW184506	10.2 $mV/m/s^2$
2	B	PCB-352C33	LW184373	10.2 $mV/m/s^2$
3	C	PCB-333B40	55350	51 $mV/m/s^2$
4	D	PCB-333B40	55354	51 $mV/m/s^2$
5	E	PCB-333B40	55353	51 $mV/m/s^2$
6	F	PCB-333B40	55351	51 $mV/m/s^2$
7	Gx	PCB-356B18	LW175704 (x)	102 $mV/m/s^2$
8	Gy	PCB-356B18	LW175704 (y)	102 $mV/m/s^2$

Table 3: DOFs notation of Figure 1a in the global coordinate system

DOF	**Cubic node**	**Axis**	**DOF**	**Cubic node**	**Axis**	**DOF**	**Cubic node**	**Axis**
1	1	x	33	11	z	65	22	y
2	1	y	34	12	x	66	22	z
3	1	z	35	12	y	67	23	x
4	2	x	36	12	z	68	23	y
5	2	y	37	13	x	69	23	z
6	2	z	38	13	y	70	24	x
7	3	x	39	13	z	71	24	y
8	3	y	40	14	x	72	24	z
9	3	z	41	14	y	73	25	x
10	4	x	42	14	z	74	25	y
11	4	y	43	15	x	75	25	z
12	4	z	44	15	y	76	26	x
13	5	x	45	15	z	77	26	y
14	5	y	46	16	x	78	26	z
15	5	z	47	16	y	79	27	x
16	6	x	48	16	z	80	27	y
17	6	y	49	17	x	81	27	z
18	6	z	50	17	y	82	28	x
19	7	x	51	17	z	83	28	y
20	7	y	52	18	x	84	28	z
21	7	z	53	18	y	85	29	x
22	8	x	54	18	z	86	29	y
23	8	y	55	19	x	87	29	z
24	8	z	56	19	y	88	30	x
25	9	x	57	19	z	89	30	y
26	9	y	58	20	x	90	30	z
27	9	z	59	20	y	91	31	x
28	10	x	60	20	z	92	31	y
29	10	y	61	21	x	93	31	z
30	10	z	62	21	y	94	32	x
31	11	x	63	21	z	95	32	y
32	11	y	64	22	x	96	32	z

were conducted under roving accelerometer conditions, one pair of accelerometers remained fixed at the DP to serve as a structural phase reference, while two additional pairs (N1 and N2) were sequentially relocated to other nodal positions. This arrangement resulted in a total of 32 distinct impact tests, as summarized in Table 4.

Each measurement consisted of eight consecutive impact events. The sampling frequency for impact tests was set at 100 samples/s. The dataset includes sequences of eight events, which were automatically cropped using a pre-trigger of 82 samples for a force threshold of 1×10^{-4} N, with logging stopping 81.9 seconds after trigger detection.

Table 4: Sequence of impact tests performed on the structure. Details regarding the input, driving point (DP), and roving accelerometer pairs (N1 and N2) are provided in Table 1, with positions (DP, N1 and N2) labeled in Figure 1.

Test	**Input**	**DP**	**N1**	**N2**	**Test**	**Input**	**DP**	**N1**	**N2**
1	+x	29	31	32	**17**	+x	29	14	15
2	+y	29	31	32	**18**	+y	29	14	15
3	+x	29	28	30	**19**	+x	29	12	13
4	+y	29	28	30	**20**	+y	29	12	13
5	+x	29	26	27	**21**	+x	29	10	11
6	+y	29	26	27	**22**	+y	29	10	11
7	+x	29	24	25	**23**	+x	29	8	9
8	+y	29	24	25	**24**	+y	29	8	9
9	+x	29	22	23	**25**	+x	29	6	7
10	+y	29	22	23	**26**	+y	29	6	7
11	+x	29	20	21	**27**	+x	29	4	5
12	+y	29	20	21	**28**	+y	29	4	5
13	+x	29	18	19	**29**	+x	29	2	3
14	+y	29	18	19	**30**	+y	29	2	3
15	+x	29	16	17	**31**	+x	29	30	1
16	+y	29	16	17	**32**	+y	29	30	1

4 Phase 2 of 2: Dynamic Testing Under Random Excitation

The second phase involved subjecting the four-story model to random excitations using the hexapod system. While the first phase exclusively considered the structure in its healthy state, this phase introduced a structural alteration during the final part of the test sequence. The damage state (d) was simulated by loosening the through bolts that secure cubes 21-25 to the third floor, thus modifying the structural integrity relative to the baseline condition.

For all tests in this phase, two acquisition sets for dynamic measurements were used simultaneously: the eight-channel DAQ (already employed in the Phase 1

for EMA) at a sampling frequency of 500 samples/s, and a second system using DMM measurements at a sampling frequency of 200 samples/s.
A univocal mapping between cubic nodes, directions, reference coordinate system and degrees of freedom (DOFs) is provided in Table 3, where DOFs are numbered from node 1 for its x, y, and z directions, up to node 32 for its x, y, and z directions.
The eight-channel DAQ involves the piezoelectric accelerometer listed in Table 2. During this phase of the test campaign, accelerometers have been displayed on the structure in three layouts, as reported in Table 5 and Figure 2. It is remarked that the sign (±) reported in Table 5 should be considered in order to obtain data records compliant with the arrows in the reference system of Figure 2.
The sequence of tests is reported in Table 6. Concerning the piezoelectric accelerometer-based setup, configuration 1 has been used for different excitation levels and directions, with the structure always in its healthy (baseline, b) state. Then, configuration 2.2 and 2.1 have been alternatively adopted considering the system as healthy (b) and damaged (d), with the excitation level and direction kept fixed.

(a) Configuration 1 (Figure 2a)

Channel	A	B	C	D	E	F	Gx	Gy
Node	29	29	25	25	17	17	1	1
(Sign) dir	(+) x	(+) y	(-) x	(+) y	(-) x	(+) y	(+) x	(+) y
DOF	85	86	73	74	49	50	1	2

(b) Configuration 2.1 (Figure 2b)

Channel	A	B	C	D	E	F	Gx	Gy
Node	26	26	25	25	27	27	1	1
(Sign) dir	(+) x	(+) y	(-) x	(+) y	(-) x	(+) y	(+) x	(+) y
DOF	76	77	73	74	79	80	1	2

(c) Configuration 2.2 (Figure 2c)

Channel	A	B	C	D	E	F	Gx	Gy
Node	26	26	25	25	28	28	1	1
(Sign) dir	(+) x	(+) y	(-) x	(+) y	(+) x	(+) y	(+) x	(+) y
DOF	76	77	73	74	82	83	1	2

Table 5: Layout of the 8 uniaxial piezoelectric accelerometers on the structure during dynamic tests under random excitation. Sensors connected to each *Channel* is indicated in Table 2, and each DOF correspond to that in Table 3. The *sign* (±) is to be considered in order to have the records compliant with the reference coordinate system, as reported in red (color version) and with arrows in Figure 2.

Table 6: Sequence of random tests on the structure using the hexapod, to be used in conjunction with Figure 2. The *structure state* is either undamaged (i.e., baseline, b) or damaged (d), where the damage consists of loosening the bolts at joint composed by cubes 21-25. While the data records with the piezoelectric accelerometer setup is always available, the DMM is not available for test 6. Test 7 consists in a repetition of test 6, where data records from both measurement systems are available. Concerning DMM, symbol (*) denotes test in which some markers have not been recorded for bad signal issues: data records of such DOFs are removed from the provided dataset.

Test	**Structure state**	**Excitation**		**Data details**	
		RMS	**Axis**	**Piezo setup**	**DMM setup**
1	b	low	x	Config. 1	Available
2	b	medium	x	Config. 1	Available
3	b	high	x	Config. 1	Available
4	b	low	y	Config. 1	Available
5	b	medium	y	Config. 1	Available
6	b	high	y	Config. 1	Not available
7	b	high	y	Config. 1	Available
8	b	low	x, y	Config. 1	Available
9	b	medium	x, y	Config. 1	Available
10	b	high	x, y	Config. 1	Available-
11	b	medium	x, y	Config. 2.1	Available
12	b	medium	x, y	Config. 2.2	Available
13	b	medium	x, y	Config. 2.1	Available(*)
14	b	medium	x, y	Config. 2.2	Available(*)
15	d	medium	x, y	Config. 2.2	Available(*)
16	d	medium	x, y	Config. 2.1	Available(*)
17	d	medium	x, y	Config. 2.1	Available(*)

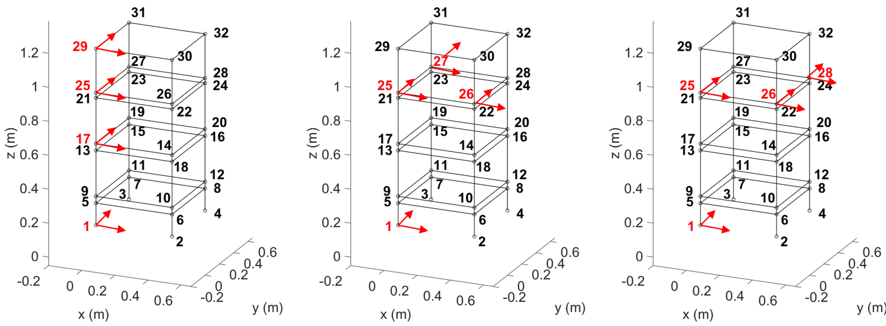

(a) Configuration 1 (b) Configuration 2.1 (c) Configuration 2.2

Figure 2: Layout of the 8 uniaxial piezoelectric accelerometers on the structure during dynamic tests under random excitation. In red (color version),the cubic node equipped with an accelerometer is highlighted. The arrows indicate the directions available in the dataset. The versus of each arrow is positive with respect to reference coordinate system: therefore, the sign indicated in Table 5 should be considered to refer to the reference coordinate system.

5 Structure of the Dataset

This section provides an overview of the organization and contents of the dataset, including the structure of the recorded data files and the associated metadata.

- **Impact Testing.** This folder contains a total of 32 MATLAB files (`.mat`), as listed in Table 4, with the corresponding metadata (`.txt`). Each file includes the following variables:
  - **Data1_A**, **Data1_B**, ..., **Data1_HAMMER**: Column vectors of the recorded signals, with labels consistent with Table 1. The values have been adjusted based on the sensitivity of each sensor.
  - **Sample rate**: A scalar value representing the sampling frequency.
  - **Data1_Ave_Count**: A scalar number corresponding to the number of impact events.
- **Dynamic Tests Under Random Excitation.** This folder is divided into two subfolders, separating the measurements obtained from piezoelectric accelerometers and those collected using the DMM.
  - **Piezoelectric Accelerometers.** This subfolder contains 17 MATLAB files (`.mat`), numbered from 1 to 17 as in Table 6, with the corresponding metadata (`.txt`). Each file includes the following variables:
    - **Data1_A**, **Data1_B**, ..., **Data1_Gy**: Column vectors of recorded signals, with labels consistent with Table 2. The values have been

pre-multiplied by the sensitivity of each sensor and are thus provided in m/s^2.

  * **Sample rate**: A scalar value representing the sampling frequency.

- **DMM.** This subfolder contains 16 MATLAB files (`.mat`) , with the corresponding metadata (`.txt`). Files are numbered from 1 to 17 as in Table 6, with Test 6 unavailable for the DMM. Thus, test 7 represents a repetition of test 6, using the same excitation in terms of RMS level and direction. Nevertheless, test 6 is included for completeness in the piezoelectric accelerometer dataset.

  Each data file contains a MATLAB *cell* variable **data**, which in turn contains each translational DOF for the 32 nodes used as target locations. According to Table 3, DOFs are numbered from node 1 for its x, y, and z directions, up to node 32 for its x, y, and z directions. Therefore, the variable **data** results from appending, in this order, the DOFs from 1 (x, y, z) to 32 (x, y, z) in a 96×1 MATLAB *cell* array.

  A DOF may be an empty cell for one of the following reasons:

  1. The corresponding node is not a DMM target, as only the 16 cubic nodes indicated in the front view of Figure 1b were equipped with a target market for DMM measurement.
  2. The quality of the DMM acquisition was deemed unacceptable. In this case, the file for that specific test is marked with an asterisk (*) in Table 6.

  The cell for a DOF with available DMM data is provided as a MATLAB *struct* with two fields:

  * **disp_raw**: Vector of recorded displacement, in meters.
  * **fsamp**: Scalar value representing the sampling frequency.

6 How to Cite This Dataset

If you use this dataset in your research or publications, please cite it as follows:

> Brambilla, M., Dertimanis, V., Chatzi, E., Chiariotti, P., & Cigada, A. (2025). *Experimental Campaign for Dynamic Characterization of a Laboratory-Scale Structure* [Dataset]. Zenodo. `https://doi.org/10.5281/zenodo.15516419`

References

[1] Kyriakos Alexandros Chondrogiannis, Vasilis Dertimanis, Boris Jeremic, and Eleni Chatzi. Design of the negative stiffness negsv mechanism for structural vibration attenuation exploiting resonance. *International Journal of Mechanical Sciences*, 260:108640, 2023.

[2] Kyriakos Alexandros Chondrogiannis, Antonios Mantakas, Moris Kalderon, Konstantinos Kapasakalis, Vasilis Dertimanis, Evangelos Sapountzakis, Ioannis Antoniadis, and Eleni Chatzi. Experimental design of the k-damper device for attenuating vibrations in structural applications. *Proceedings of the World Conference on Earthquake Engineering 2024 (WCEE 2024)*, 2024.